Inhibition of mineral dissolution by aggregation of colloidal particles driven by diffusiophoresis

Sophie Roman, Flore Rembert

Letter

Inhibition of mineral dissolution by aggregation of colloidal particles driven by diffusiophoresis

Sophie Roman* and Flore Rembert
ISTO, UMR 7327, Université Orleans, CNRS, BRGM, OSUC, F-45071 Orléans, France

(Received 22 September 2024; revised 24 November 2024; accepted 15 January 2025; published 18 March 2025)

This letter presents a new mechanism of interaction between mineral dissolution and colloidal transport. Using microfluidic experiments, we demonstrate that diffusiophoresis, i.e., the motion of colloidal particles due to solute concentration gradients, offers an appealing solution to drive colloidal particles toward a dissolving mineral. We report that particle aggregation limits the mineral dissolution through the formation of a passivation layer around the mineral. This work could be exploited to turn undesirable mechanisms (e.g., dissolution of confinement barriers and release of toxic components by contaminants trapped in porous formations) into positive feedback as the concentration gradients resulting from these events become the driving force to deliver colloids for remediation.

DOI: 10.1103/PhysRevFluids.10.L032501

Introduction. Many subsurface engineering applications foresaw the usage of colloidal particles for groundwater remediation or for sealing damaged geological confinement barriers [1,2]. The injection of nanoparticles (reactive or adsorptive) into contaminated porous media (soil, sediments, aquifers) is gaining attention in remediation technologies. Despite their great potential, injecting colloids in subsurface reservoirs is challenging as the delivery of the reactive materials to the contaminated or damaged regions is not well controlled [3]. Unlike well-known fluid and particle transport processes driven by gradients of pressure, gravity, or electromagnetic potential, diffusiophoretic transport of charged particles is only driven by chemical concentration gradients without the application of any external field. The mechanisms and theory behind diffusiophoresis are now well described. Electrolytic diffusiophoresis is the result of (i) chemiphoresis that refers to particle motion due to the osmotic pressure gradient over the particle surface (ii) and electrophoresis due to the macroscopic electric field generated by an ionic gradient as a result of the difference in the diffusivities of the cations and anions [4]. Nonelectrolytic diffusiophoresis is due to chemiphoresis only [5]. Colloidal migration generated by diffusiophoresis can be up to three orders of magnitude faster than pure diffusion (up to 10^{-5} m/s), thus likely to be critical in various processes in porous media [6,7]. Several studies have shown the importance of diffusiophoresis in explaining mechanisms for which consensus could not be reached. For example, in biophysics, Alessio and Gupta (2023) demonstrated the role of diffusiophoresis in Turing patterns [8], and Haefner and Muller (2024) showed that intracellular organization could depend on reaction-driven diffusiophoresis [9].

Using microfluidic experiments, diffusiophoretic effects have been explored to control colloid transport in and out of dead-end pores [7,10,11], to separate colloidal particles [10,12], or to

*Contact author: sophie.roman@univ-orleans.fr

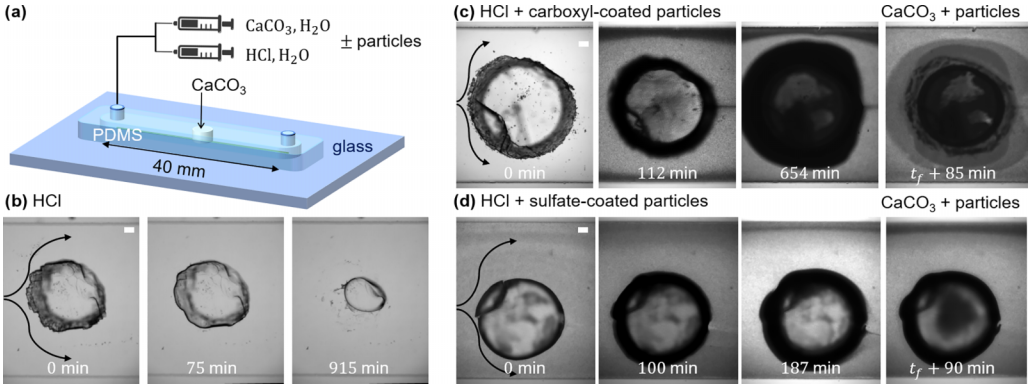

FIG. 1. (a) Experimental setup. (b) Images of injection experiments at 2 µL/min of 0.02_{wt}% HCl without particles, (c) with carboxyl-coated polystyrene particles, (d) with sulfate-coated particles. From $t = 0$ min the acid solution is injected for 1020 min (t_f) [(b),(c)] or 240 min (t_f) (d), then the $CaCO_3$ saturated solution with particles is injected for 90 min to stop the reaction. Most carboxyl-coated particles are detached from the calcite grain after the reaction [(c), at $t_f + 85$ min] while the aggregate made of sulfate-coated particles remains attached to the calcite [(d), at $t_f + 90$ min]. The scale bar in white is 100 µm.

trap particles or macromolecules [13]. In most of these studies, the application of an external concentration gradient is used. However, in a natural environment, concentration gradients are produced locally by physicochemical processes. Some studies use an *in situ* source of concentration gradient to drive colloids. For example, a solute concentration gradient source that emits a steady flux of solute over long time scales has been designed [14,15], or calcium carbonate dissolution is used as a source of concentration gradient for diffusiophoresis [16]. The use of *in situ* sources of a concentration gradient has been described for pure diffusive conditions mainly, whereas in natural porous media various flow conditions are encountered. We hypothesize that in conditions representative of subsurface environments, particle trajectories can deviate from the pressure-driven flow using mineral dissolution as a source of concentration gradient.

Method. We use a piece of calcite ($CaCO_3$), a widely distributed mineral, of about 900 µm in diameter and 150 µm thick, sealed in the middle of a microfluidic channel 1.5 mm wide, 150 µm deep, and 40 mm long, see Fig. 1(a). The calcite undergoes dissolution under acidic conditions, leading to a concentration gradient of dissolved species around the calcite. This microfluidic setup, used in [17–19], is relevant to subsurface geochemical processes to probe couplings between fluid flow and reactivity. The microchannel is saturated either with water in equilibrium with calcium carbonate, thus not leading to mineral dissolution (pH = 7.8), or with a solution of 0.02_{wt}% hydrochloric acid (HCl) leading to the dissolution of the grain (pH = 2.3), Fig. 1(b). The primary chemical reaction that affects calcium carbonate during dissolution is as follows:

$$CaCO_{3(s)} + H^+_{(aq)} \rightleftharpoons Ca^{2+}_{(aq)} + HCO^-_{3(aq)}.$$

To study the effect of a local source of concentration gradient on colloid flow, the aqueous solutions are seeded with colloidal particles made of polystyrene, 1 µm in diameter (Polysciences). Different surface coatings are tested, carboxyl and sulfate-coating lead to negatively charged particles, and amine groups lead to positive charges. To assess if diffusiophoresis has an impact when the flow is dominated by advection compared to diffusion, we use an imposed flow rate of 2 µl/min and of 0 µl/min, respectively. This gives a Péclet number of $Pé = \frac{w \times u}{D} = 31$, and $Pé = 0$, with w the width of the channel, u the mean velocity of the fluid, and D the diffusion coefficient of protons. All experiments are performed with and without the chemical reaction. Details of experimental procedures are presented in Supplemental Material A [20].

TABLE I. Mean dissolution and particle aggregation rates measured from experiments for a flow of 0.02_{wt}% HCl at 2 μL/min.

Particles	Dissolution rate (10^{-4} min^{-1})	Aggregation rate (10^{-3} min^{-1})
No	10.9	0.0
Carboxyl coated	0.3	3.6
Sulfate coated	0.0	2.1

Results. First, we explore flow conditions dominated by advection. When acid is injected without particles, the dissolution of the calcite grain, see Fig. 1(b), follows the same trends as in Soulaine *et al*. (2017), see also Movie S1 in Supplemental Material B [20]. The shape of the dissolving calcite is influenced by the hydrodynamics in the channel with a lower local dissolution rate upstream at the stagnant zone of the flow [17]. From image processing of the top view of the calcite grain, we determine a mean dissolution rate of 10.9×10^{-4} min^{-1}. The dissolution rate is related to the initial calcite size and the measurement method is explained in Supplemental Material A [20].

When the injected acid is seeded with positively charged particles (i.e., coated with amine groups) the same behavior is observed without or with dissolution of the calcite, particles are flowing around the calcite with no visible interaction of the particles with the calcite, see Supplemental Material E [20]. The pH of the acid solution is 6.5 in this case, indeed for lower pH the amine-coated particles tend to form aggregates and sediment. At pH 6.5, we measured the dissolution rate of calcite at 1.30×10^{-7} min^{-1} for 20 h of reaction.

We report the formation of an aggregate of particles around a dissolving mineral when negatively charged particles are seeded in the acid solution and flow around the calcite grain. The pH in this case is 2.3. Pictures of the aggregates are presented in Figs. 1(c) and 1(d), and videos are shown in Movies S2, S3, and S4 (Supplemental Material B [20]). We hypothesize that the focusing of particles around the calcite is driven by diffusiophoresis due to the concentration gradients generated by the mineral dissolution. For carboxyl-coated particles, the HCl solution seeded with particles is injected at 2 μL/min for 17 h, then the $CaCO_3$ saturated solution is injected for 90 min at the same flow rate. In this case, we observed a continuous growth of the aggregate made of particles, see Fig. 1(c). Our observations suggest that carboxyl-coated particles form an unbound aggregate around the calcite that permits acid to flow through the calcite surface, and as the reaction is going on the aggregate keeps growing. Thus the source of the concentration gradient is maintained over long periods and plays the role of a collector for the particles. This phenomenon is reversible, indeed when the reaction is stopped most of the aggregate is displaced from the calcite surface, see Fig. 1(c) at $t_f + 85$ min. For sulfate-coated particles, we also observed the formation of an aggregate made of particles, however, it stopped growing after 3 h 20 min. In this case, the HCl solution seeded with particles is injected at 2 μL/min for 4 h, then the $CaCO_3$-saturated solution is injected for 90 min at the same flow rate. In this case, the aggregate made of particles is consolidated and does not grow indefinitely. The dense aggregate does not allow the acid to react with the calcite after 188 min, thus stopping the reaction and the release of dissolved species. For sulfate-coated particles, the phenomenon is irreversible: The aggregated particles remain in place and act as a permanent passivation layer, even after replacing the acid injection by the $CaCO_3$-saturated solution, see Fig. 1(d), at $t_f + 90$ min. The different particle aggregation dynamics are further discussed in Supplemental Material C [20]. In this work, in addition to driving and aggregating particles toward an *in situ* source of concentration gradient [7,10,11], we observe the formation of a passivation layer made of the particles that neutralizes the source of dissolved species.

In Table I, we present the measurements of the dissolution rate of calcite and the rate of aggregation of particles. Measurement methods are detailed in Supplemental Material A [20]. The mean aggregation rate of particles is in the same order of magnitude for carboxyl- and sulfate-coated particles at about 3×10^{-3} min^{-1}. Interestingly, this aggregation of particles affects the dissolution rate

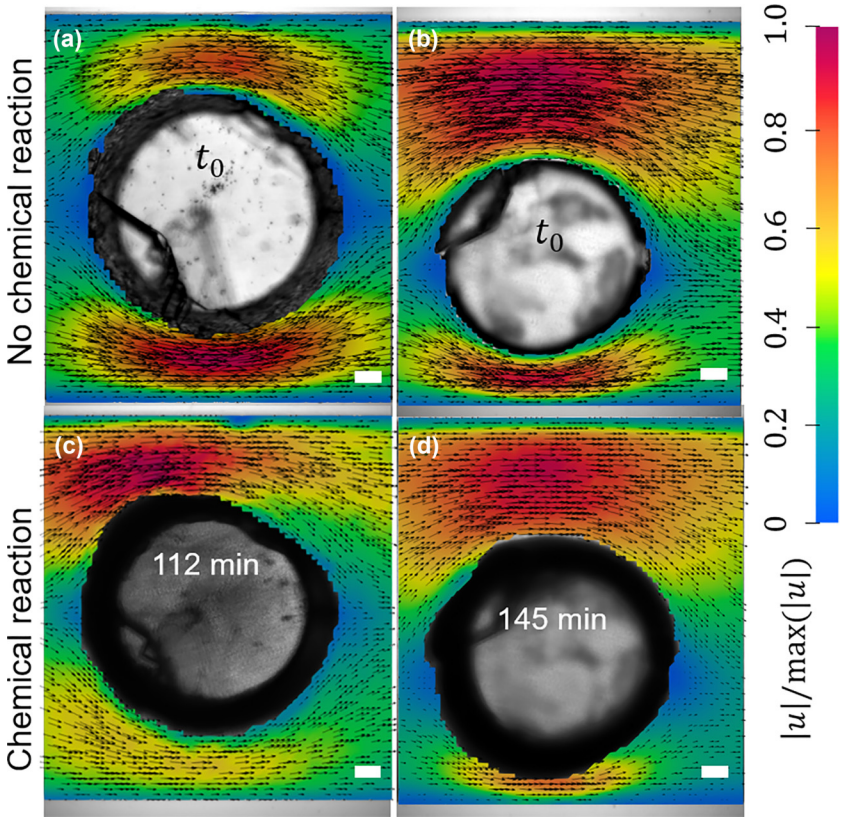

FIG. 2. Velocity magnitude of particles measured by micro-PIV without calcite dissolution [(a),(b)] and with dissolution [(c),(d)] and for different particle coatings, carboxyl [(a),(c)], and sulfate [(b),(d)]. All velocities are normalized by the maximum velocity in the channel. Time t_0 is without chemical reaction and particles are suspended in the $CaCO_3$ solution. The minutes indicated in the second row correspond to the time elapsed since the acid injection. The scale bars are 100 μm.

of calcite. For carboxyl-coated particles, the average dissolution rate is $0.3 \times 10^{-4}\,\mathrm{min}^{-1}$; it is more than one order of magnitude slower than dissolution without particle injection. In this case, the particle aggregate creates a physical barrier that limits the access to the calcite surface for the acid, thus slowing down the dissolution. When sulfate-coated particles seeded in an acid solution are injected, the calcite dissolution rate is estimated at zero. Indeed, the dense aggregate formed around the calcite prevents its dissolution. Li *et al.* (2015) demonstrated the protective effect of sulfate against acid attack by sulfate adsorption and/or coating of $CaSO_4$ on $CaCO_3$ grains [21]. Thus the suppression of dissolution by sulfate-coated particles is most probably driven by a chemical mechanism.

We demonstrated that mineral dissolution can be inhibited by injecting particles that form a passivation layer around the mineral. Negatively charged particles move toward the local source of the concentration gradient. For this system, we were unable to capture the displacement of the particles toward the calcite because of the presence of strong advective flux. In Fig. 2, we present particle velocity fields measured by micro-PIV (particle image velocimetry) [22,23] for carboxyl-coated [(a), (c)], and sulfate-coated particles [(b), (d)], without chemical reaction [(t_0: (a), (b)] or during [$t = 112, 145$ min, Figs. 2(c) and 2(d), respectively]. Particle velocity fields show the classic Stokes flow behavior with streamlines that follow the shape of the calcite. The mean velocity in the channels is around 150 μm/s, thus two orders of magnitude greater than theoretical diffusiophoretic velocity values [24]. To further assess the role of diffusiophoresis in our system, suspensions of

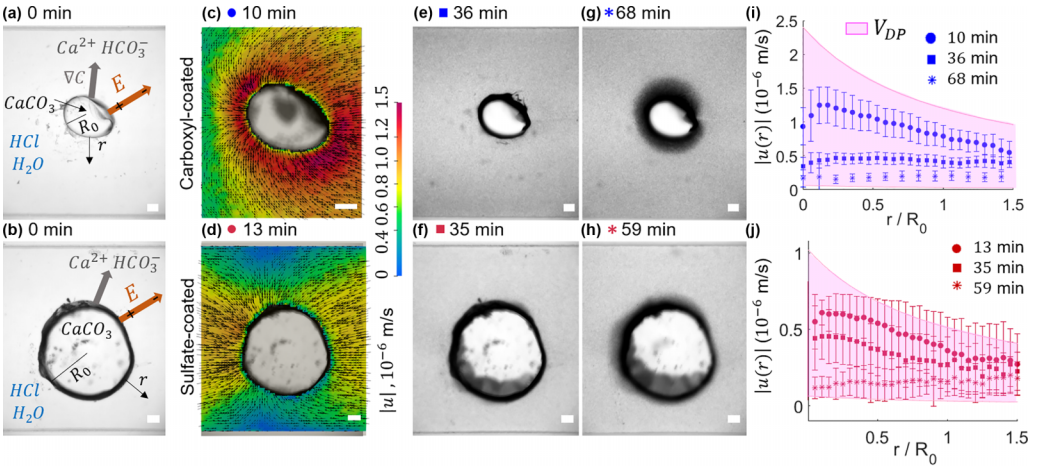

FIG. 3. Negatively charged particle around a dissolving calcite with no imposed flow. (a) and (b) microchannel containing a calcite crystal suspended in the HCl solution before colloid injection. Diffusiophoresis around the dissolving calcite mineral is schematized, the electric field and concentration gradient are oriented radially outward to the calcite. R_0 is the radius of the calcite, and r is the radial position. From $t > 0$ minute carboxyl-coated particles [(c),(e),(g),(i)] or sulfate-coated particles [(d),(f),(h),(j)] are injected. (c) and (d) velocity fields of particles measured by micro-PIV after 10 min and 13 min. Snapshots of the calcite surrounded by carboxyl-coated particles after 36 min (e) and 68 min (g), and by sulfate-coated particles after particles 35 min (f) and 59 min (h). Mean radial velocity profiles for carboxyl-coated particles (i) and sulfate-coated particles (j) for different times after particle injection. V_{DP} is the theoretical diffusiophoretic velocity as a function of r for the two extreme pH values in the system. Scale bars are 100 μm.

particles in an acid solution have been put in contact with a calcite grain with no imposed flow to suppress advective flux that prevents the measurement of diffusiophoresis.

In Fig. 3, we present the results for pure diffusive conditions. First, we discuss the expected diffusiophoretic behavior of particles in the presence of a radial concentration profile of species. In our experiments, the primary ions produced during the dissolution are Ca^{2+}, and HCO_3^-, and they have a higher concentration near the dissolving calcite than farther away, resulting in a concentration gradient of dissolved species in the radial direction of the calcite [16], see Figs. 3(a) and 3(b). These ions have different diffusion coefficients, at 20 °C $D_{Ca^{2+}} = 7.92 \times 10^{-10}$ m^2/s and $D_{HCO_3^-} = 1.19 \times 10^{-9}$ m^2/s [25]. The difference in diffusivities leads to an electric field generated to maintain the electroneutrality that is oriented radially outward from the calcite, see Fig. 3. Thus, negatively charged particles are attracted to the dissolving calcite. The diffusiophoretic velocity of particles, V_{DP}, is expressed following [26–28]

$$V_{\mathrm{DP}} = \Gamma_{\mathrm{DP}} \times \frac{\nabla C}{C}, \tag{1}$$

with the diffusiophoretic mobility

$$\Gamma_{\mathrm{DP}} = \frac{\epsilon kT}{\mu Ze}\left\{\beta\zeta_p - \frac{2kT}{Ze} \times \ln\left(1 - \tanh^2\left(\frac{Ze\zeta_p}{4kT}\right)\right)\right\}, \tag{2}$$

with C the concentration of the electrolyte, kT the thermal energy, e the electron charge, Z the valence of the electrolyte, ϵ the permittivity of the medium, μ its viscosity, ζ_p the zeta potential of the particles, and $\beta = \frac{D_+ - D_-}{D_+ + D_-}$ the difference in diffusivity of the primary ions. We consider the concentration gradient of produced species, assuming an initial bath concentration of zero, we have $\frac{\nabla C}{C} = -\frac{1}{r}$, with r the radial position from the center of the calcite, see analysis by Banerjee *et al.*

[14] and McDermott *et al.* [16]. We assume that the change in the calcite size due to dissolution is much slower than the change in the concentration of produced species. In our system, ζ_p depends on the coating at the surface of the particles and on the position of the particle in the channel (ζ_p depends on local concentrations of H^+) [29,30].

First, we consider the case of colloids for which the diffusiophoretic effect is negligible as a control experiment. For amine-coated particles (positively charged), $\zeta_p = 30 - 55\,\text{mV}$ for the pH range $2.3 - 7.8$ [30], this leads to velocities of $V_{DP} = 1.2 \times 10^{-7}$ to $2.6 \times 10^{-7}\,\text{m/s}$. These low values show that diffusiophoresis is negligible in this case. This is supported by our observations. For pure diffusive conditions, with and without chemical reaction, we observe only Brownian motion for amine-coated particles, with no preferential direction, see Movie S5 in Supplemental Material B [20]. When advection is dominant in our system, the injection of amine-coated particles during calcite dissolution does not lead to particle aggregation around the mineral for several hours of acid injection.

For pure diffusive conditions, negatively charged particles seeded in the acid solution show a motion toward the dissolving calcite, as shown by the velocity vectors plotted in Figs. 3(c) and 3(d), pictures of the calcite surrounded by particles in Figs. 3(e) and 3(f), and Movie S6 in Supplemental Material B [20]. After about 60 min, most of the particles diffuse away from the calcite where they were accumulated, Figs. 3(g) and 3(h). In Figs. 3(i) and 3(j), the area in pink represents the theoretical V_{DP} values. They are determined as a function of r for the extreme values of ζ_p, i.e., corresponding to pH = 2.3 and pH = 7.8. From the literature, we chose ζ_p between $-5\,\text{mV}$ at low pH and $-65\,\text{mV}$ at greater pH for carboxyl-coated particles [29], and between $-10\,\text{mV}$ and $-65\,\text{mV}$ for sulfate-coated particles [31]. In experiments, the concentration gradient vanishes with time leading to a time-dependent speed of the particles. However, to estimate if the experimental speed of our particles agrees with the diffusiophoretic velocity, we consider theoretically a time-independent diffusiophoretic behavior. We also plotted the experimental radial velocities of particles averaged over the entire observation window for different times after the injection of particles. Each point corresponds to the mean value and standard deviation of $u(r)$ for all positions r in the channel (radial position from the edge of the calcite). The motion of the particles is constrained in the vertical direction by the channel walls, thus explaining the large standard deviations during the diffusiophoretic motion. At the beginning of the reaction [10 and 13 min, circles in Figs. 3(i) and 3(j)] carboxyl- and sulfate-coated particles show absolute radial velocities up to $1.3 \times 10^{-6}\,\text{m/s}$ and $5.8 \times 10^{-7}\,\text{m/s}$, respectively, which are two to 10 times greater than for amine-coated particles and lead to remarkable diffusiophoretic aggregation. The velocity of particles slightly decreases with increasing distance from the calcite. These velocity profiles are in range and trend with the theoretical diffusiophoretic velocities. After about 30 min [Figs. 3(i) and 3(j), squares] velocity values are intermediate, showing a decrease in the diffusiophoretic effect with time. Sixty min after the particle injection, the velocity of carboxyl- and sulfate-coated particles is low [$<2 \times 10^{-7}\,\text{m/s}$, Figs. 3(i) and 3(j), stars], and does not depend on the radial position, showing no diffusiophoretic effect anymore. The effect of the concentration gradient generated by the chemical reaction on particle flow lasts between 30 min and 60 min. This is in agreement with the dynamic of diffusion of Ca^{2+}, and HCO_3^- in our system. Numerical simulations show that it takes about 40 min to reach saturation concentrations in the channel, see Supplemental Material D [20]. The concentration gradient vanishes at saturation, thus impeding any diffusiophoretic behavior. In Mc Dermott *et al.* (2012), the movement of the particles toward or away from a dissolving mineral was observed, however, no accumulation of particles around the minerals is reported. This is probably because the size of the minerals is close to the size of the particles in their case, thus not offering enough reactive surface area for the particles to bond to the calcite [16]. To the best of our knowledge, it is the first time that particle aggregation due to diffusiophoresis around a reactive mineral is observed. The study of pure diffusive conditions demonstrates the role of diffusiophoresis in forming the aggregate. In the advective case, the continuous injection of the acid preserves the concentration gradient (see numerical simulations, Supplemental Material D [20]), thus driving particles by diffusiophoresis for long periods.

Conclusion. In this work, we demonstrated that diffusiophoretic effects can drive particles toward a source of concentration gradient and lead to the formation of a passivation layer around the source of dissolved species. It opens new lines of research to limit the release of potentially harmful chemicals in water, or to prevent mineral reaction. When diffusion is dominant in our system (Fig. 3), the diffusiophoretic motion of negatively charged particles toward a dissolving mineral is measured and agrees with theoretical predictions. When advection is dominant (Figs. 1 and 2), velocities in the channel are two orders of magnitude greater than diffusiophoretic velocities. In these conditions, particles in the vicinity of the source of concentration are driven by diffusiophoresis, while particles away from it are only driven by advection. As the acid solution is constantly injected, the concentration gradient is maintained around the dissolving mineral, allowing for a large aggregate to form. Depending on the chemical groups at the surface of the particles, the aggregate is either unconsolidated or dense. For the unconsolidated case, the chemical reaction is slowed down and the dissolving mineral acts like a collector with long-lasting behavior. By injecting sulfate-coated particles, a dense aggregate is chemically formed, which stops the reaction permanently. These findings confirm the protective effect of sulfate on calcareous materials against acid attack [21]. Here, we demonstrate the possibility to specifically transport sulfate materials toward carbonated layers to harness their protective power. In natural environments, by choosing particle coating or particle material in agreement with the chemical process of interest, it is possible to design chemical reaction controllers using diffusiophoretic systems [32]. The potential importance of diffusiophoresis in natural and biological environments for various processes has been highlighted previously [33,34]. This work further demonstrates that mineral dissolution could be a driving mechanism in geological porous media. Besides subsurface environments, particles driven by concentration gradients in porous media are useful for biomedical applications like bone-crack repair using drug-loaded particles [35] or drug delivery [36].

Acknowledgments. This research was funded by the European Union (ERC, TRACE-it, Grant Agreement No. 101039854), the French National Research Agency (ANR) on the LabEx VOLTAIRE (Grant No. ANR-10-LABX-100-01). The authors thank Kali Dézert for the preliminary experiments and preparation of the calcite grains. The authors would like to thank the GREMI laboratory (UMR7344) for access to its cleanroom facilities for microfabrication.

Data Availability. The data that support the findings of this article are openly available [37], embargo periods may apply.

[1] A. C. Mitchell, A. J. Phillips, R. Hiebert, R. Gerlach, L. H. Spangler, and A. B. Cunningham, Biofilm enhanced geologic sequestration of supercritical CO_2, Int. J. Greenhouse Gas Control **3**, 90 (2009).

[2] C. Tsakiroglou, K. Terzi, A. Sikinioti-Lock, K. Hajdu, and C. Aggelopoulos, Assessing the capacity of zero valent iron nanofluids to remediate NAPL-polluted porous media, Sci. Total Environ. **563–564**, 866 (2016).

[3] T. Zhang, G. V. Lowry, N. L. Capiro, J. Chen, W. Chen, Y. Chen, D. D. Dionysiou, D. W. Elliott, S. Ghoshal, T. Hofmann, H. Hsu-Kim, J. Hughes, C. Jiang, G. Jiang, C. Jing, M. Kavanaugh, Q. Li, S. Liu, J. Ma, B. Pan *et al.*, In situ remediation of subsurface contamination: Opportunities and challenges for nanotechnology and advanced materials, Environ. Sci.: Nano **6**, 1283 (2019).

[4] J. T. Ault, S. Shin, and H. A. Stone, Diffusiophoresis in narrow channel flows, J. Fluid Mech. **854**, 420 (2018).

[5] J. L. Anderson, Colloid transport by interfacial forces, Annu. Rev. Fluid Mech. **21**, 61 (1989).

[6] B. Abecassis, C. Cottin-Bizonne, C. Ybert, A. Ajdari, and L. Bocquet, Boosting migration of large particles by solute contrasts, Nat. Mater. **7**, 785 (2008).

[7] A. Kar, T.-Y. Chiang, I. Ortiz Rivera, A. Sen, and D. Velegol, Enhanced transport into and out of dead-end pores, ACS Nano **9**, 746 (2015).

[8] B. M. Alessio and A. Gupta, Diffusiophoresis-enhanced turing patterns, Sci. Adv. **9**, eadj2457 (2023).
[9] G. Häfner and M. Müller, Reaction-driven diffusiophoresis of liquid condensates: Potential mechanisms for intracellular organization, ACS Nano **18**, 16530 (2024).
[10] S. Shin, E. Um, B. Sabass, J. T. Ault, M. Rahimi, P. B. Warren, and H. A. Stone, Size-dependent control of colloid transport via solute gradients in dead-end channels, Proc. Natl. Acad. Sci. USA **113**, 257 (2016).
[11] S. Battat, J. T. Ault, S. Shin, S. Khodaparast, and H. A. Stone, Particle entrainment in dead-end pores by diffusiophoresis, Soft Matter **15**, 3879 (2019).
[12] T. J. Shimokusu, V. G. Maybruck, J. T. Ault, and S. Shin, Colloid separation by CO_2-induced diffusiophoresis, Langmuir **36**, 7032 (2020).
[13] J. Palacci, C. Cottin-Bizonne, C. Ybert, and L. Bocquet, Osmotic traps for colloids and macromolecules based on logarithmic sensing in salt taxis, Soft Matter **8**, 980 (2012).
[14] A. Banerjee, I. Williams, R. N. Azevedo, M. E. Helgeson, and T. M. Squires, Soluto-inertial phenomena: Designing long-range, long-lasting, surface-specific interactions in suspensions, Proc. Natl. Acad. Sci. USA **113**, 8612 (2016).
[15] A. Banerjee and T. M. Squires, Long-range, selective, on-demand suspension interactions: Combining and triggering soluto-inertial beacons, Sci. Adv. **5**, eaax1893 (2019).
[16] J. J. McDermott, A. Kar, M. Daher, S. Klara, G. Wang, A. Sen, and D. Velegol, Self-generated diffusioosmotic flows from calcium carbonate micropumps, Langmuir **28**, 15491 (2012).
[17] C. Soulaine, S. Roman, A. Kovscek, and H. A. Tchelepi, Mineral dissolution and wormholing from a pore-scale perspective, J. Fluid Mech. **827**, 457 (2017).
[18] C. Soulaine, S. Roman, A. Kovscek, and H. A. Tchelepi, Pore-scale modelling of multiphase reactive flow: application to mineral dissolution with production of CO_2, J. Fluid Mech. **855**, 616 (2018).
[19] F. Rembert, A. Stolz, C. Soulaine, and S. Roman, A microfluidic chip for geoelectrical monitoring of critical zone processes, Lab Chip **23**, 3433 (2023).
[20] See Supplemental Material at http://link.aps.org/supplemental/10.1103/PhysRevFluids.10.L032501 for detailed materials and methods, descriptions of movies, discussion of the aggregation dynamics, numerical results of the concentration profiles around a dissolving calcite, and discussion on the injection of amine-coated particles.
[21] Q. Li, Y. M. Lim, and Y.-S. Jun, Effects of sulfate during CO_2 attack on portland cement and their impacts on mechanical properties under geologic CO_2 sequestration conditions, Environ. Sci. Technol. **49**, 7032 (2015).
[22] S. Roman, C. Soulaine, M. AbuAlSaud, A. Kovscek, and H. Tchelepi, Particle velocimetry analysis of immiscible two-phase flow in micromodels, Adv. Water Resour. **95**, 199 (2016).
[23] W. Thielicke and E. Stamhuis, PIVlab - Towards user-friendly, affordable and accurate digital particle image velocimetry in MATLAB, J. Open Res. Software **2**, e30 (2014).
[24] D. C. Prieve, J. L. Anderson, J. P. Ebel, and M. E. Lowell, Motion of a particle generated by chemical gradients. Part 2. Electrolytes, J. Fluid Mech. **148**, 247 (1984).
[25] D. R. Lide, *CRC Handbook of Chemistry and Physics* (CRC press, Boca Raton, 2004), Vol. 85.
[26] J. L. Anderson, M. Lowell, and D. Prieve, Motion of a particle generated by chemical gradients Part 1. Non-electrolytes, J. Fluid Mech. **117**, 107 (1982).
[27] B. Derjaguin, S. Dukhin, and A. Korotkova, Diffusiophoresis in electrolyte solutions and its role in the mechanism of the formation of films from caoutchouc latexes by the ionic deposition method, Prog. Surf. Sci. **43**, 153 (1993).
[28] S. Marbach, H. Yoshida, and L. Bocquet, Local and global force balance for diffusiophoretic transport, J. Fluid Mech. **892**, A6 (2020).
[29] H. Al-Shehri, T. Horozov, and V. Paunov, Adsorption of carboxylic modified latex particles at liquid interfaces studied by the gel trapping technique, Soft Matter **10**, 6433 (2014).
[30] P. Marmey, N. Lebaz, M. Eissa, T. Delair, and A. Elaissari, Polystyrene latex particles bearing primary amine groups via soap-free emulsion polymerization, Polym. Int. **69**, 1038 (2020).
[31] O. Oriekhova and S. Stoll, Investigation of $FeCl_3$ induced coagulation processes using electrophoretic measurement, nanoparticle tracking analysis and dynamic light scattering: Importance of pH and colloid surface charge, Colloids Surf. A **461**, 212 (2014).

[32] N. Shi, R. Nery-Azevedo, A. I. Abdel-Fattah, and T. M. Squires, Diffusiophoretic focusing of suspended colloids, Phys. Rev. Lett. **117**, 258001 (2016).
[33] D. Velegol, A. Garg, R. Guha, A. Kar, and M. Kumar, Origins of concentration gradients for diffusiophoresis, Soft Matter **12**, 4686 (2016).
[34] B. Ramm, A. Goychuk, A. Khmelinskaia, P. Blumhardt, H. Eto, K. A. Ganzinger, E. Frey, and P. Schwille, A diffusiophoretic mechanism for ATP-driven transport without motor proteins, Nat. Phys. **17**, 850 (2021).
[35] V. Yadav, J. D. Freedman, M. Grinstaff, and A. Sen, Bone-crack detection, targeting, and repair using ion gradients, Angew. Chem. Int. Ed. **52**, 10997 (2013).
[36] N. Singh, G. Vladisavljević, F. Nadal, C. Cottin-Bizonne, C. Pirat, and G. Bolognesi, Reversible trapping of colloids in microgrooved channels via diffusiophoresis under steady-state solute gradients, Phys. Rev. Lett. **125**, 248002 (2020).
[37] S. Roman and F. Rembert, Data for "inhibition of mineral dissolution by aggregation of colloidal particles driven by diffusiophoresis" Zenodo (2025), doi:10.5281/zenodo.14697632.